

Laser induced modulation of the Landau level structure in single-layer graphene

Alexander López^{1,*}, Antonio Di Teodoro¹, John Schliemann², Bertrand Berche³, and Benjamin Santos⁴

1. School of Physics Yachay Tech, Yachay City of Knowledge 100119-Urcuqui, Ecuador

2. Institute for Theoretical Physics, University of Regensburg, D-93040 Regensburg, Germany

3. Statistical Physics Group, Institut Jean Lamour[†],
CNRS – Université de Lorraine – Campus de Nancy,

B.P. 70239, F - 54506 Vandœuvre lès Nancy Cedex, France, EU

4. INRS-EMT, Université du Québec, 1650 Lionel-Boulet, Varennes, Québec J3X 1S2, Canada

(Dated: April 14, 2019)

We present perturbative analytical results of the Landau level quasienergy spectrum, autocorrelation function and out of plane pseudospin polarization for a single graphene sheet subject to intense circularly polarized terahertz radiation. For the quasienergy spectrum, we find a striking non trivial level-dependent dynamically induced gap structure. This photoinduced modulation of the energy band structure gives rise to shifts of the revival times in the autocorrelation function and it also leads to modulation of the oscillations in the dynamical evolution of the out of plane pseudospin polarization, which measures the angular momentum transfer between light and graphene electrons. For a coherent state, chosen as an initial pseudospin configuration, the dynamics induces additional quantum revivals of the wave function that manifest as shifts of the maxima and minima of the autocorrelation function, with additional partial revivals and beating patterns. These additional maxima and beating patterns stem from the effective dynamical coupling of the static eigenstates. We discuss the possible experimental detection schemes of our theoretical results and their relevance in new practical implementation of radiation fields in graphene physics.

PACS numbers: 78.67.Wj, 71.70.Di, 72.80.Vp

I. INTRODUCTION

The dynamical control of the transport properties of Dirac fermions in the condensed matter realm is currently an intense research topic. These Dirac fermions have been shown to emerge as the low energy excitations of two-dimensional systems with a honeycomb lattice structure as it occurs in graphene¹⁻³. Recent theoretical⁴⁻⁶ and experimental⁷ works have discussed the role of radiation fields in the manipulation of the transport properties of monolayer graphene samples. By focusing on the Terahertz frequency regime particular attention is paid to the tunability of the induced band gaps. In addition, the possibility of generating topological insulating behavior was theoretically put forward both in the static⁸ and dynamical regimes.⁹⁻¹¹

In presence of a perpendicular quantizing magnetic field $\mathbf{B} = B\hat{z}$, the static spectrum of single layer graphene possesses a \sqrt{B} field dependence which strikingly contrasts the linear B dependence for conventional non relativistic 2DEG¹. In addition, the $n = 0$ Landau level (LL) has only one sublattice occupied at each Dirac point. Considering the LL scenario and a topological contribution given by an excitonic gap the authors of reference¹² predict the appearance of Rabi oscillations when the system's initial quantum state is prepared by means of a short electric pulse and the subsequent dynamics is controlled by the oscillations between the dynamically coupled LL.

In this work we theoretically analyze the dynamical manipulation of the LL structure of charge carriers on suspended monolayer graphene when a periodically driving radiation field is applied perpendicular to the sample. A similar set up was proposed in reference¹³, where a laser field is introduced via the dipolar approximation. In that work, the authors discuss the dynamics of *Zitterbewegung* which is described in terms of the radiation field emitted by the accelerated charge carriers in graphene. In our proposal we make use of Floquet's theorem to recast the dynamics in an explicitly time-independent fashion but without need to resort to infinite-dimensional Fourier-mode expansion. Our approach has the advantage of providing an analytical description of the driven evolution of relevant physical quantities as the pseudospin polarization which is a measure of the angular momentum exchange among the charge carriers and the radiation field¹⁴. In the following we explicitly show how our semi analytical results are relevant at high values of the quantizing magnetic field B , where the coupling to the radiation field leads to non trivial qualitative modifications of the dynamical behavior of relevant physical quantities within the perturbative regime.

The paper is organized as follows. In section II we present the model and summarize the perturbative results for the quasienergy spectrum. In section III we study the dynamics of the autocorrelation function and pseudospin polarization for two initially prepared states. First we consider an eigenstate of the static Hamiltonian that has vanishing pseudospin polarization in the static regime. Next, we present the same analysis for an initially prepared coherent state, with static finite pseudospin polarization and highlight the main differences with respect to

[†]Laboratoire associé au CNRS UMR 7198

the other initial configuration. In section IV we discuss our main results and in section V we present concluding remarks and argue on the experimental implementation of our proposed theoretical setup. Finally, in the appendix we summarize some mathematical calculations arising during the perturbative analysis.

II. MODEL

In this section we focus on the low energy properties of non interacting spinless charge carriers in a suspended monolayer graphene subject to a perpendicular, uniform and constant magnetic field $\mathbf{B} = B\hat{z}$. The dynamics is governed by Dirac's Hamiltonian. In coordinate representation it reads ($\hbar = 1$)

$$\mathcal{H}_\eta(\mathbf{r}) = v_F(\eta\pi_x\sigma_x + \pi_y\sigma_y), \quad (1)$$

where $v_F \sim 10^6 m/s$ is the Fermi velocity in graphene. In addition, the canonical momenta $\pi_j = k_j + eA_j$ ($j = x, y$) contain the vector potential ($\nabla \times \mathbf{A} = \mathbf{B}$), $-e$ is the electronic charge ($e > 0$), and $\eta = \pm 1$ describes the valley degree of freedom. Using the definition of the magnetic length $l_B^{-2} = eB$ and the cyclotron energy $\omega_c = \sqrt{2}v_F/l_B$ the Hamiltonian Eq. (1) at each K (K') Dirac point, which corresponds to $\eta = +1$ ($\eta = -1$), can be written in the form

$$H^{+1} = \omega_c \begin{pmatrix} 0 & a \\ a^\dagger & 0 \end{pmatrix} \quad (2)$$

$$H^{-1} = -\omega_c \begin{pmatrix} 0 & a^\dagger \\ a & 0 \end{pmatrix} \quad (3)$$

where the annihilation and creation operators are defined by standard relations as

$$a = \frac{l_B(\pi_x - i\pi_y)}{\sqrt{2}} \quad \text{and} \quad a^\dagger = \frac{l_B(\pi_x + i\pi_y)}{\sqrt{2}}.$$

The eigenenergies of the Hamiltonian (1) are then

$$E_n^{s,\eta} = s\eta\sqrt{n}\omega_c \quad (4)$$

with $s = \pm 1$. Positive (negative) values of $s\eta$ represents the conduction (valence) band at each Dirac point. In addition, the integer quantum number $n = 0, 1, 2 \dots$ labels the Landau level (LL) structure of monolayer graphene. Using the eigenstates $|n\rangle$ of the operator $a^\dagger a$, the corresponding eigenstates $|\varphi_n^{s,\eta}\rangle$ read

$$|\varphi_n^{s,+1}\rangle = \frac{1}{\sqrt{2}} \begin{pmatrix} s|n-1\rangle \\ |n\rangle \end{pmatrix} \quad (5)$$

$$|\varphi_n^{s,-1}\rangle = \frac{1}{\sqrt{2}} \begin{pmatrix} -s|n\rangle \\ |n-1\rangle \end{pmatrix} \quad (6)$$

for $n \neq 0$. The zero energy eigenstate ($n = 0$) is given in each case by

$$|\varphi_0^{+1}\rangle = \begin{pmatrix} 0 \\ |0\rangle \end{pmatrix} \quad (7)$$

$$|\varphi_0^{-1}\rangle = \begin{pmatrix} |0\rangle \\ 0 \end{pmatrix}. \quad (8)$$

Due to time-reversal symmetry, we have $\mathcal{T}H^{+1}\mathcal{T} = H^{-1}$. Let us now consider the effect of intense circularly polarized terahertz electromagnetic radiation, incident perpendicularly to the sample. We assume that the beam radiation spot is large enough compared to the lattice spacing so we can neglect any spatial variation. According to the standard light-matter interaction formulation, the dynamical effects of a monochromatic radiation field incident perpendicular to the sample can be described by means of a time-dependent vector potential

$$\mathbf{A}(t) = \frac{\mathcal{E}}{\omega} (\cos \omega t, \delta \sin \omega t), \quad (9)$$

where \mathcal{E} and ω are respectively the amplitude and frequency of the electric field given in turn by the standard relation $\mathcal{E}(t) = -\partial_t \mathbf{A}(t)$. In addition, we are using $\delta = +1$ ($\delta = -1$) for right (left) circular polarization. We are using circular polarization because it has been shown to provide the maximal photoinduced bandgap¹⁵. Starting from the ordinary dipolar interaction term $-e\mathbf{k}\cdot\mathbf{A}(t)$, introduced to the Tight-Binding Hamiltonian via the Peierls substitution, we can evaluate the effects of the driving at each Dirac point as

$$V^\eta = ev_F[\eta\sigma_x A_x(t) + \delta\sigma_y A_y(t)], \quad (10)$$

which explicitly reads

$$V^\eta = \xi\eta(\sigma_x \cos \omega t + \eta\delta\sigma_y \sin \omega t). \quad (11)$$

with the effective coupling constant $\xi = ev_F\mathcal{E}/\omega$. This makes the total Hamiltonian

$$H^\eta(t) = H^\eta + V^\eta(t), \quad (12)$$

periodic in time $H^\eta(t+T) = H^\eta(t)$, with $T = 2\pi/\omega$ the period of oscillation of the driving field. Therefore, if we focus on the K Dirac point ($\eta = 1$), the physics at the K' Dirac point ($\eta = -1$) can be easily found by the substitutions $\xi \rightarrow -\xi$ and $\omega \rightarrow -\omega$.

Thus, let us focus on the K point physics and afterwards, we can make the necessary substitutions. In order to simplify the notation we set $H^{+1} = H_0$ and $V^{+1}(t) = V(t)$. Hence, defining rising σ_+ and lowering σ_- pseudospin operators by the standard formulas

$$\sigma_\pm = \frac{\sigma_x \pm i\sigma_y}{2},$$

the time-dependent interaction potential can be rewritten as

$$V(t) = \xi(e^{-i\delta\omega t}\sigma_+ + e^{i\delta\omega t}\sigma_-), \quad (13)$$

Now we invoke Floquet's theorem which states that the time evolution operator of the system induced by a periodic Hamiltonian can be written in the form¹⁶

$$U(t) = P(t)e^{-iH_F t}, \quad (14)$$

with $P(t)$ a periodic unitary matrix and H_F a time-independent dynamical generator referred to as the

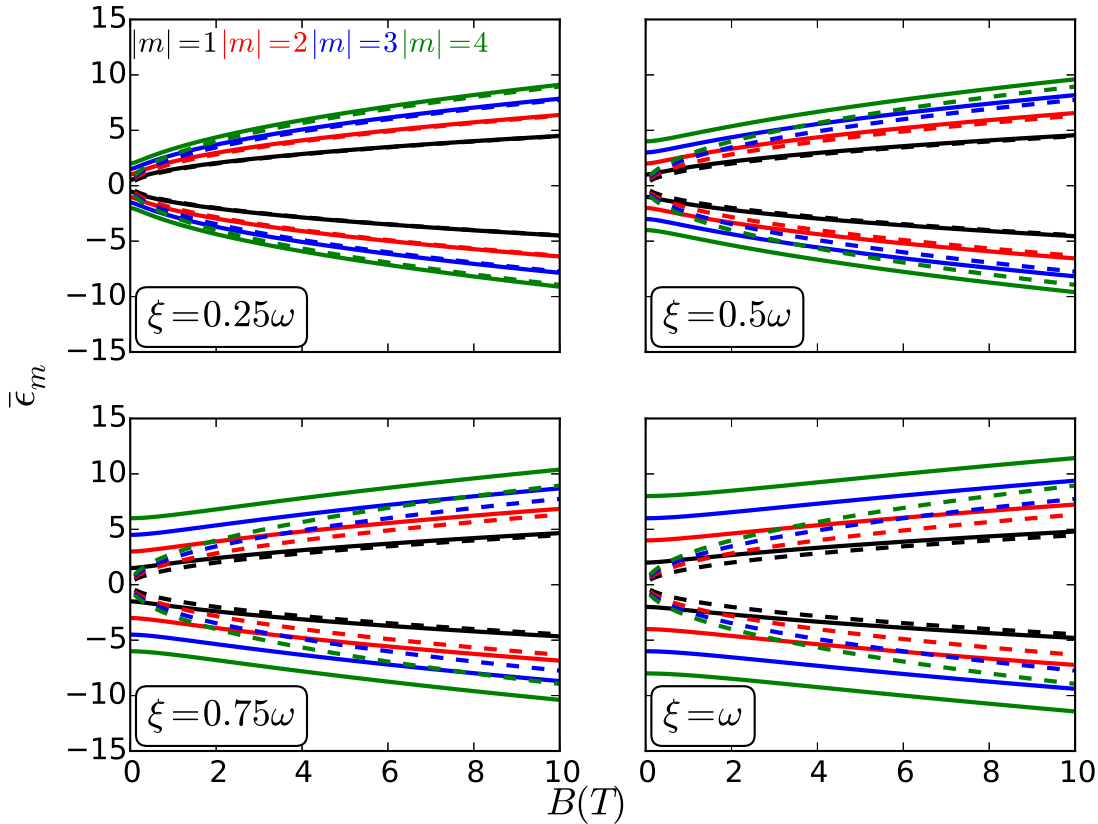


FIG. 1: (Color online) Approximate mean energies for the driven scenario (continuous lines) as function of the quantizing magnetic field B . The dotted lines represent the undriven spectra for the corresponding LL. We notice a level-dependent energy gap that leads to non trivial behavior of physical quantities, as discussed below (see main text).

Floquet Hamiltonian. The eigenvalues of the Floquet Hamiltonian H_F represent the quasienergy spectrum of the periodically driven system. Typically, in order to solve for the quasienergy spectrum, one can expand each term of the time-dependent Schrödinger equation in Fourier space and numerically solve an infinite eigenvalue problem. Instead, we will take a perturbative approach as discussed below.

Accordingly, for our problem we can find approximate solutions to the dynamics by modifying slightly the analytical strategy presented in¹⁷. Then, one finds that the excitation number operator N_a , defined as

$$N_a = \left(a^\dagger a + \frac{1}{2} \right) \mathbb{1} + \frac{\sigma_z}{2}, \quad (15)$$

which commutes with the Hamiltonian H_0 and satisfies the eigenvalue equation

$$N_a |\varphi_n^s\rangle = n |\varphi_n^s\rangle. \quad (16)$$

N_a generates a time-dependent unitary transformation $|\Psi(t)\rangle = P(t)|\Phi(t)\rangle$ given as

$$P(t) = \exp(-iN_a \delta \omega t), \quad (17)$$

such that the time-dependent Schrödinger equation

$$i\partial_t |\Psi(t)\rangle = H(t) |\Psi(t)\rangle \quad (18)$$

can be transformed with a time-independent operator H_F governing the dynamics of the problem

$$i\partial_t |\Phi(t)\rangle = H_F |\Phi(t)\rangle, \quad (19)$$

where H_F and $|\Phi(t)\rangle$ are the Floquet Hamiltonian and Floquet eigenstate, respectively. Doing the explicit calculation, H_F is found to be given by

$$H_F = H_0 - N_a \delta \omega + \xi \sigma_x. \quad (20)$$

In the following we focus on recent experiments in the far infrared frequency domain⁷ for which $\omega \approx 10$ meV. In addition, we consider values of the electric field intensities⁶ $\mathcal{E} \sim 0.15$ MV/m. Then one gets for the coupling constant $\xi \approx 10$ meV which, for frequencies ω in the terahertz domain leads to $\xi \approx \omega$. This is an order of magnitude smaller than the Landau level separation $\omega_c \approx 116$ meV, for $B = 10$ T. For larger frequencies and stronger magnetic field intensities, the ratio ξ/ω_c

tends to be smaller. Therefore, we can perform a perturbative treatment in the effective coupling parameter $\lambda = \xi/\omega_c < 1$.

For this purpose we transform the Hamiltonian (20) as $H = e^{(\lambda/2)I_-} H_F e^{-(\lambda/2)I_-}$, where we have introduced the antihermitian operator $I_- = a^\dagger \sigma_- - a \sigma_+$. Evaluating up to first order we get

$$H \approx H_F + \frac{\lambda}{2} [I_-, H_F]. \quad (21)$$

Evaluation of the commutator gives (in the appendix we summarize the explicit derivations)

$$[I_-, H_F] = -\omega_c [2N_a + \lambda(a^\dagger + a)] \sigma_z, \quad (22)$$

and defining the shifted operator $b = a + \lambda$ one gets, to leading order in λ , the effective Hamiltonian

$$H = \omega_c (b^\dagger \sigma_- + b \sigma_+) - \delta\omega N_b - \xi N_b \sigma_z, \quad (23)$$

where we have introduced the shifted number operator

$$N_b = b^\dagger b + \frac{1 + \sigma_z}{2}.$$

In equation (23) we have neglected the additive higher order terms

$$\Delta V = \omega \lambda (b^\dagger + b) - \lambda^2 \omega, \quad (24)$$

which can be dealt with by higher order perturbation theory. Thus, the approximate quasienergies are found to be given as

$$\epsilon_m^s = s\omega_c \sqrt{m} \sqrt{1 + m\lambda^2}, \quad \text{mod } \omega, \quad (25)$$

which can be rewritten as

$$\epsilon_m^s = s\sqrt{m\omega_c^2 + (m\xi)^2}, \quad \text{mod } \omega. \quad (26)$$

Then, to this order of approximation, all quasienergies corresponding to the $m \neq 0$ LL are shifted, whereas the $m = 0$ remains insensitive to the radiation field and agrees with the result reported in reference¹⁸ for bilayer graphene. Yet, a more detailed derivation by means of second order perturbation theory shows that there is a small $O(\lambda^4)$ energy correction due to first non-diagonal terms in equation (24) which couple all adjacent LL. This higher order corrections could be important at low quantizing magnetic fields for which the condition $\lambda = \xi/\omega_c \approx 1$ could be satisfied.

Let us now analyze some physical consequences of the radiation field on the Landau level structure of monolayer graphene with focus on the interplay among the quantizing magnetic field and the light-matter interaction. To begin with, we notice that the quasienergies are defined up to multiples of ω ; therefore, a better physical characterization of the energy spectrum for the driven system is provided by the mean energies¹⁶

$$\bar{\epsilon}_m^s = \epsilon_m^s - \omega \frac{\partial \epsilon_m^s}{\partial \omega}, \quad (27)$$

which are invariant under $\epsilon_m^s \rightarrow \epsilon_m^s + l\omega$, for l being an integer. Doing the explicit calculation the mean energies are found to be given by the expression

$$\bar{\epsilon}_m^s = s \left(\frac{m\omega_c^2 + 2m^2\xi^2}{\sqrt{m\omega_c^2 + m^2\xi^2}} \right), \quad (28)$$

where we remember the definition of the effective coupling to the radiation field as $\xi = ev_F \mathcal{E}/\omega$.

As can be seen in FIG. 1, these mean energies are plotted as function of the quantizing magnetic field B , for different values of the Landau level index changing the effective coupling ξ . We notice that, at intermediate light-coupling strength, the energy resolution of these levels becomes much better and could experimentally be tested for not so large quantizing magnetic fields B . Moreover, we find that to this order of approximation the LL become gapped, with the striking feature that the photoinduced gap is level dependent. These gap openings appear except for the shifted $m = 0$ level which, as discussed before, remains insensitive to the radiation field.

Below we will deal with the photoinduced dynamical features and therefore, we give the corresponding normalized Floquet eigenstates for $m \neq 0$

$$|\psi_m^s\rangle = \begin{pmatrix} s f_m^{-s} |m-1\rangle \\ f_m^s |m\rangle \end{pmatrix}, \quad (29)$$

where we have defined the coefficients

$$f_m^s = \sqrt{\frac{\epsilon_m + sm\xi}{2\epsilon_m}}, \quad (30)$$

with $\epsilon_m = |\epsilon_m^s|$. In addition, the zero energy shifted eigenstate ($m = 0$) is still given by $|\varphi_0\rangle$, i. e.,

$$|\psi_0\rangle = \begin{pmatrix} 0 \\ |0\rangle \end{pmatrix}. \quad (31)$$

III. PSEUDOSPIN AND AUTOCORRELATION FUNCTION DYNAMICS

Now that we have found the approximate Floquet eigenstates and quasienergies, we explore other dynamical features of the driven LL configuration by evaluating the mean values of the pseudospin polarization operator and its relation to the autocorrelation function dynamics¹⁹.

For this purpose, let us first assume that the system is initially prepared in an eigenstate of the Hamiltonian H_0

$$|\Psi(0)\rangle = |\varphi_m^s\rangle, \quad (32)$$

with $m \neq 0$. In the Floquet basis (29), the initial state is written as

$$|\varphi_m^s\rangle = \sum_{s'=\pm s} D_m^{ss'} |\psi_m^{s'}\rangle, \quad (33)$$

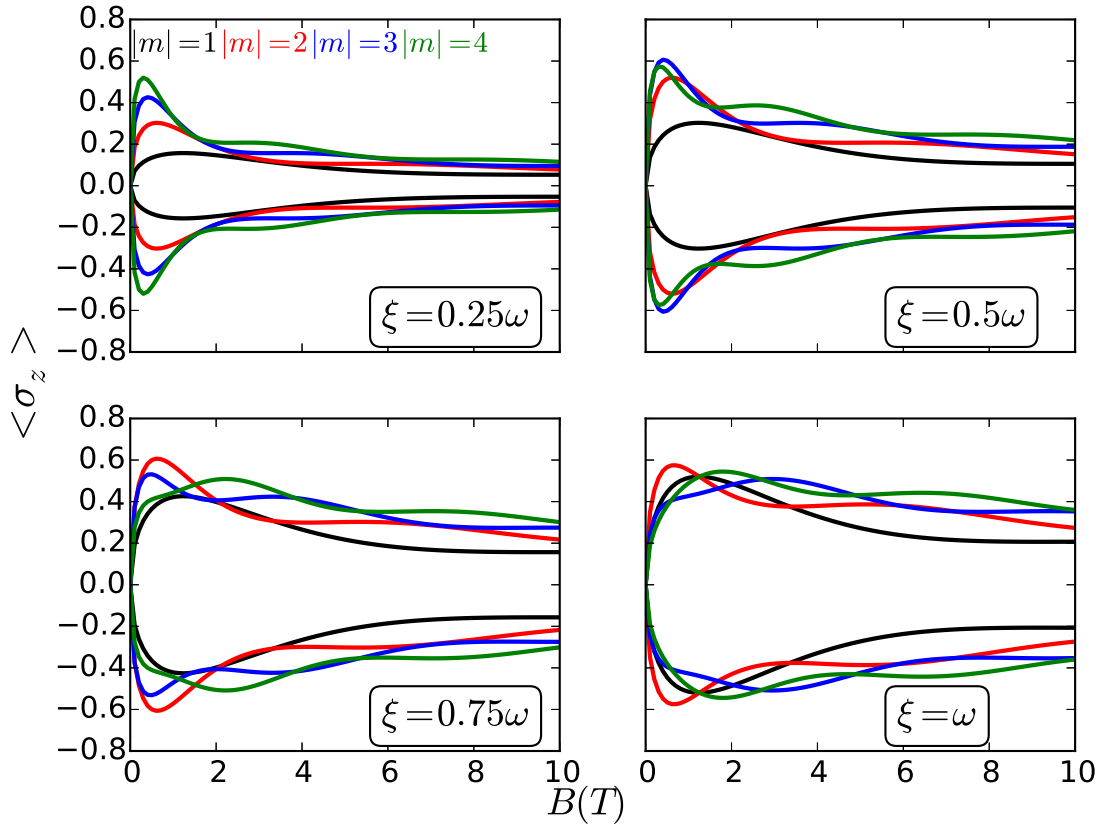


FIG. 2: (Color online) Approximate mean pseudospin polarization $\langle \sigma_z \rangle$ for the driven scenario as given by equation (39), plotted as a function of the quantizing magnetic field B . We have selected the first four LL $m = 1, \dots, 4$, at four values of the light-matter coupling strength. The lower panels show that at large magnetic fields ($B = 10$ T) both the $m = 3$ and $m = 4$ LL pseudospin polarization still remains degenerate. Hence higher order perturbation terms should be necessary in order to lift this degeneracy.

where the expansion coefficients are given by

$$D_m^{ss'} = \frac{1}{\sqrt{2}} \left(f_m^{s'} + ss' f_m^{-s'} \right). \quad (34)$$

Taking into account that the $|\psi_{\pm m}\rangle$ states are degenerate eigenstates of N_b , the unitary operator $e^{-iN_b \omega t}$ would just contribute a phase $e^{-i\omega m t}$. Using the Hamiltonian (23) the evolved state can be written as

$$|\Psi(t)\rangle = \sum_{s'=\pm s} D_m^{ss'}(t) e^{-is'\epsilon_m t} |\psi_m^{s'}\rangle, \quad (35)$$

where we have introduced the time-dependent coefficients $D_m^{ss'}(t) = D_m^{ss'} e^{-i\omega m t}$. Let us then consider the dynamics for the autocorrelation function and pseudospin polarization $\sigma_z(t)$ operators from which we can respectively infer the feasibility of manipulating the polarization state of the sample and the dipole moment radiation emitted by the driven sample. It is important to remark at this point that studying the out of plane pseudospin polarization is a means of

detecting the angular momentum exchange between the Dirac fermions in graphene and the circularly polarized radiation field, as can be inferred from the discussion in the recent literature about the role of σ_z in describing the total angular momentum content of the system¹⁴.

With these ideas in mind, we first begin by evaluating the pseudospin polarization

$$\sigma_z(t, \xi) = \langle \Psi(t) | \sigma_z | \Psi(t) \rangle. \quad (36)$$

For the chosen initial state we find $\sigma_z(t, 0) = 0$. When expression (36) is evaluated we find after some algebraic manipulations

$$\sigma_z(t, \xi) = \frac{2s\sqrt{m^3}\xi\omega_c}{\epsilon_m^2} \sin^2 \epsilon_m t. \quad (37)$$

We note that for vanishing values of the coupling to the radiation field $\xi \rightarrow 0$ one has $\sigma_z(t, 0) = 0$. Therefore, once the electromagnetic field is present the pseudospin

oscillations are a manifestation of the angular momentum exchange among the radiation field and the charge carriers in graphene¹⁴.

As discussed in the case of the quasienergies, we could better quantify the effects of the driving field by evaluating the average

$$\langle \sigma_z \rangle = \frac{1}{T} \int_0^T dt \sigma_z(t, \xi), \quad (38)$$

with the period of the radiation field given as $T = 2\pi/\omega$. Then we get the expression

$$\langle \sigma_z \rangle = \frac{s\sqrt{m^3}\xi\omega_c}{\epsilon_m^2} (1 - \text{sinc } 2\epsilon_m T), \quad (39)$$

with $\text{sinc } x = \sin x/x$.

In figure FIG.2 we plot the behavior of $\langle \sigma_z \rangle$ as a function of the coupling strength ξ . At small $\xi = 0.25\omega$ we see that the closer the state is to the $m = 0$ LL the role of the radiation field in modifying its pseudospin polarization is less relevant and this is correlated to the fact that, within this regime, the gap openings seen in the mean quasienergy spectrum are not so noticeable at different values of the m LL index. In addition, at large values of the quantizing field, $B = 10T$, the value of the pseudospin polarization is almost the same at each value of the m LL index. However, we see in the second upper panel that already at intermediate values of the relative coupling strength $\xi = 0.5\omega$ that at large values of the quantizing field $B = 10T$ one can discern among the different LL polarization value which serves to separate each level contribution to this quantity dynamical behavior. In the lower two panels we show that this physical picture becomes more obvious at larger values of ξ , with perfect separation for the contribution from the $m = 1$ and $m = 2$, levels. Yet, the corresponding $m = 3$ and $m = 4$ contributions to the pseudospin polarization remain degenerate at large B values. One would expect that this degeneracy could be removed by including higher order perturbative contributions, since then the coupling among nearby levels would lead to additional splittings in the quasienergy spectrum that would in turn also lift the pseudospin degeneracy.

In order to discuss more general dynamical features, one should consider a superposition state. However, in order to do so we must take into account the feasibility of experimentally realizing such a superposition state. A paradigmatic case of such interesting superposition states is given by the coherent state which are minimal uncertainty wave packets relevant for studying the classical states of the radiation field in the sense of being a classical counterpart of the quantum harmonic oscillator. Since, as in the quantum harmonic oscillator, the Landau levels in graphene are eigenstates of the number operator, one should expect that these coherent state superpositions would be interesting. Indeed, there has been recently

some proposals to analyze the dynamics of coherent electronic states in graphene nanomechanical resonators²⁰. By taking advantage of the intrinsic non linear nature of flexural modes in graphene, the authors of reference²⁰ show that cat-like²¹ states can be generated. We follow a different physical approach. Instead of resorting to nonlinearities of flexural modes we invoke the light-matter coupling as a mechanism for studying the evolution of an initially prepared coherent superposition state built from the Landau level eigenstates described in section I and evaluate the induced pseudospin polarization effects in order to contrast to the results shown in FIG.2. Formally speaking, the coherent state $|\alpha\rangle$ is defined by means of the eigenvalue equation

$$A|\alpha\rangle = \alpha|\alpha\rangle, \quad (40)$$

where $A = a\mathbb{1}$. Using the expansion

$$|\alpha\rangle = c_0|\varphi_0\rangle + \sum_{sn} \bar{c}_n^s |\varphi_n^s\rangle, \quad (41)$$

with \sum_{sn} representing a summation for all $n \neq 0$. Assuming, without loss of generality, the symmetric scenario $c_n^{-s} = c_n^s$, one finds that the coherent state is given as

$$|\alpha\rangle = e^{-\frac{|\alpha|^2}{2}} \left(|\varphi_0\rangle + \frac{1}{\sqrt{2}} \sum_{sn} \frac{\alpha^n}{\sqrt{n!}} |\varphi_n^s\rangle \right), \quad (42)$$

which can be shown to be normalized. In this case, we find

$$\langle \alpha | \sigma_z(t) | \alpha \rangle = -e^{-|\alpha|^2} \sum_n \frac{|\alpha|^{2n}}{n!} \left(\frac{\omega_c^2 \cos 2\epsilon_n t + |n|\xi^2}{\omega_c^2 + |n|\xi^2} \right) \quad (43)$$

This is plotted in FIG. 3 for $\xi = 0.25$ and four representative values of α . In this figure we notice that for small values of α the dynamics of the pseudospin polarization resembles the pattern for Rabi oscillations since the main contributions would arise for the interference among the zero and first LL. Yet, no polarization inversion can be achieved within this regime.

However, once $\alpha = 1$ the contribution from other LL states becomes increasingly important to the interference pattern and the former Rabi oscillations become distorted. Moreover, at this value of α , one can achieve the polarization inversion for large enough values of time in the long-term evolution. In the lower panels of FIG. 4 we find that for larger values ($\alpha = 4$ and $\alpha = 8$), we get a beating pattern showing a dynamical localization effect that is directly related to a collective behavior of the driven charge carriers in graphene.

This physical picture for the coherent state dynamics can be complemented by studying the autocorrelation function $C_\alpha(t) = \langle \alpha | \Psi(t) \rangle$, which is found to be given as

$$C_\alpha(t) = e^{-|\alpha|^2} \sum_n \frac{|\alpha|^{2n}}{n!} \left(\cos \epsilon_n t + i \frac{n\xi}{\epsilon_n} \sin \epsilon_n t \right). \quad (44)$$

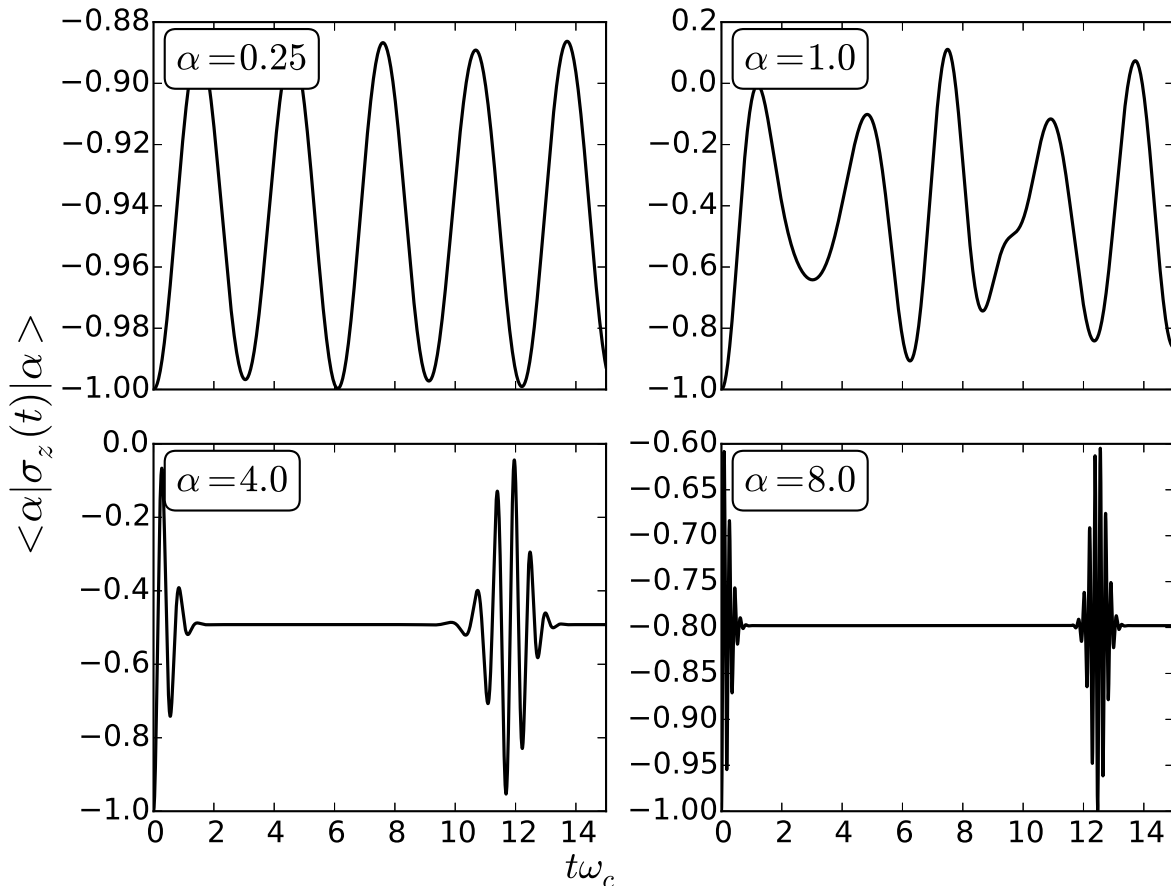


FIG. 3: Time dependence of the pseudospin polarization as given in equation (43). The panels show the dynamical behavior at four characteristic values of the parameter α . For the numerical evaluation of the series we have truncated at $n = N = 100$. The upper panels show the coherence among the lowest LL whereas the lower panels show localization effects approaching the classical behavior, which corresponds to large values of α . See the discussion in the main text.

Its time evolution is plotted in FIG.4 choosing again an effective coupling strength value of $\xi = 0.25\omega_c$ and the same values of α as in FIG.3 showing the dynamical behavior of the pseudospin polarization. Comparing FIG.3 and FIG.4 we see that partial revivals for the autocorrelation function are correlated to the beating or localization behavior of the pseudospin polarization. Therefore, one could indirectly gain information on the pseudospin dynamics by measuring the time revivals¹⁹ which means detecting those times for which the wave packet reconstructs itself. In order to show explicitly the role of the driving field we have plotted in FIG. 5 the static autocorrelation function. Comparing the lower right panels in FIG. 4 and FIG. 5, we find that the radiation field induces additional revivals in accordance to the beating pattern in the pseudospin oscillation, as seen in FIG.3.

IV. DISCUSSION

We have shown that the radiation field leads to a quasienergy spectrum with a level dependent gap, except for the $m = 0$ LL which, to leading order, remains insensitive to the radiation field effects. In addition, we have found that a finite out of plane pseudospin polarization value can arise for initial states that possess either a finite or vanishing initial value of σ_z . As we saw at the beginning of section (II) in presence of the radiation field, the total out of plane angular momentum component j_z of the electrons is no longer a constant of motion. Therefore, the pseudospin oscillations are due to the angular momentum exchange among the driving field and the charge carriers in single layer graphene. For the coherent state a beating pattern emerges in the pseudospin polarization. In spite of the fact that the interaction is dictated by a periodic Hamiltonian we find that the dominant or characteristic time scale for this collective behavior is the cyclotron frequency. We could expect this behavior of the wave packet at large values of α as

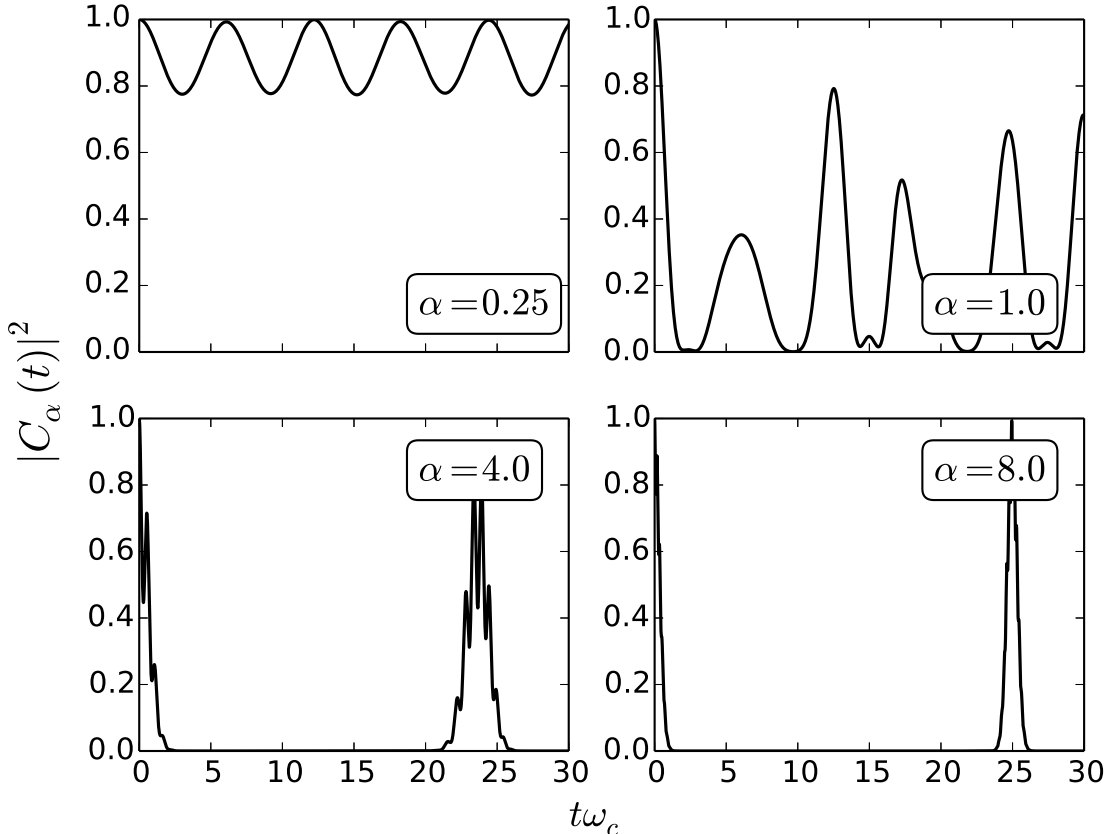


FIG. 4: Time dependence of the autocorrelation function as given by the square of expression in equation (44), truncated at $n = N = 100$. For large $\alpha = 4$ and $\alpha = 8$, it is the cyclotron frequency ω_c instead of the driving frequency ω which determines the time scale for the revival times. Comparing to FIG.3 it is apparent that information on the pseudospin dynamics can be indirectly inferred from the autocorrelation function dynamics. See discussion in the main text.

a measure of the classical behavior associated to the cyclotron problem but now realized with Dirac fermions in the LL quantized regime as was discussed by one of the authors in reference²². We must remark that in order to be able to detect the reported effects an ensemble of coherent states should be prepared each time, because the measurement process destroys the state. It should also be remembered that the coherent state parameter α is determined by choosing appropriate values for the mean values of position and momentum in accordance to the following prescription

$$\langle \alpha | x | \alpha \rangle = \ell_B \Re(\alpha), \quad (45)$$

$$\langle \alpha | p_x | \alpha \rangle = \frac{1}{\ell_B} \Im(\alpha). \quad (46)$$

Another point to be highlighted is that for standard two dimensional electron gases the coherent state built from the Landau levels would remain coherent, i.e., it would evolve in time in such a manner that it would just oscillate in time around the prescribed mean values given in eqs. (45) and (46). More precisely, its Wigner function

representation in phase space will oscillate in time without deformation. This is known to be a consequence of the fact that the dependence with the n quantum number is linear. Yet, in graphene we have a \sqrt{n} and this in turn prevents the coherent state to evolve in such a coherent manner.

Therefore, the spreading of the wave packet and the corresponding appearance of the additional revival times a shorter time values is a direct consequence of the driving field that even at low coupling can induced interesting dynamical behavior as shown in FIG.3 and FIG.4. We supported this last statement by evaluating the static ($\xi = 0$) autocorrelation function as shown in FIG. 5 and found that the second packet reconstruction (see lower panel for $\alpha = 8$ in FIG.4) around $t\omega_c \approx 25$ is absent in the static regime.

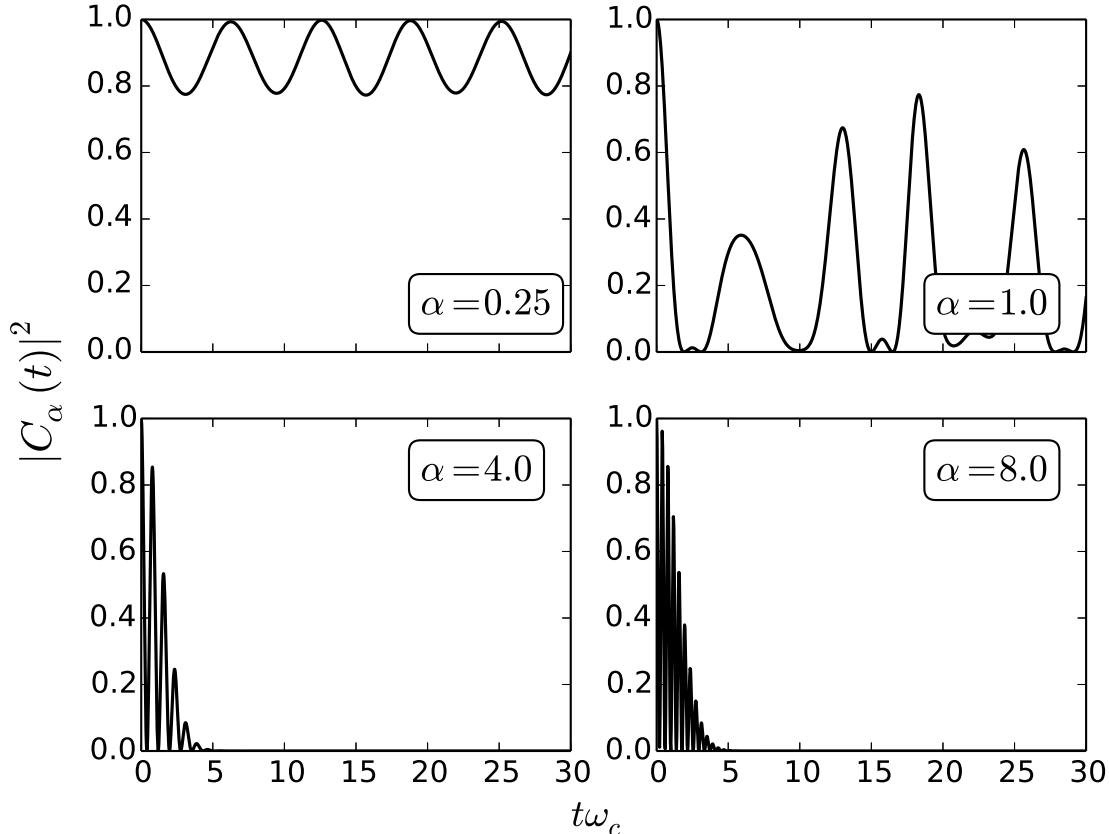


FIG. 5: Time dependence of the autocorrelation function as given in equation (48) truncated at $n = N = 100$ in absence of radiation field $\xi = 0$. In the upper panels we see that at small values of $\alpha = 0.25$ and $\alpha = 1$, the static and driven autocorrelation function are qualitatively similar. Yet, the photoinduced quantum revivals at larger times are not seen in the two lower panels as compared to those panels in FIG.4

V. CONCLUSIONS

We have analyzed the dynamical modulation of physical quantities for Dirac fermions within the Landau level quantized regime of single layer graphene subject to intense circularly polarized terahertz radiation. By means of a perturbative analytical treatment we found very interesting physical features such as a non trivial level dependent dynamically induced gap structure. Due to the angular momentum exchange among the radiation field and the charge carriers, it also leads to modulation of the oscillations in the dynamics of the out of plane pseudospin polarization, even for superposition states with an initially vanishing pseudospin value. We also found that localization effects in the time evolution of the pseudospin polarization can be keep track of by measuring the revival times of a wave packet initially prepared as a coherent state. The reported photoinduced gap modulation and pseudospin oscillations could be detected through the reemitted dipolar radiation from the oscillating charge carriers as it was proposed in

reference¹³.

Acknowledgments– This work has been supported by Deutsche Forschungsgemeinschaft via GRK 1570 and Yachay Tech via the project “Non dissipative transport in honeycomb lattice materials: Interplay of spin-orbit interaction, radiation fields and superconductivity”. AL thanks the University of Lorraine for partial financial support through research visits. BB thanks Yachay Tech for financial support for research visits.

VI. APPENDIX

A. Perturbative calculation of effective Hamiltonian for single layer graphene

In order to get the effective Hamiltonian for single layer graphene we need to evaluate the following expression

$$H = e^{\lambda/2I_-} H_F e^{-\lambda/2I_-}, \quad (47)$$

with the antihermitian operator

$$I_- = \hat{a}^\dagger \sigma_- - \hat{a} \sigma_+. \quad (48)$$

Using the Baker Campbell Hausdorff formula we have

$$H = H_F + \frac{\lambda}{2} [I_-, H_F] + \frac{1}{2!} \left(\frac{\lambda}{2} \right)^2 [I_-, [I_-, H_F]] + \dots \quad (49)$$

The first commutator is worked out explicitly

$$[I_-, H_F] = [\hat{a}^\dagger \sigma_- - \hat{a} \sigma_+, H_F]. \quad (50)$$

Since $H_F = \omega_c I_+ - \omega \hat{N}_a + \xi \sigma_x$ and $[I_-, \hat{N}_a] = 0$, with $I_+ = \hat{a}^\dagger \sigma_- + \hat{a} \sigma_+$, we only need to evaluate two commutators. The first one gives

$$\begin{aligned} [I_-, I_+] &= [\hat{a}^\dagger \sigma_- - \hat{a} \sigma_+, \hat{a}^\dagger \sigma_- + \hat{a} \sigma_+] \\ &= -2[\hat{a} \sigma_+, \hat{a}^\dagger \sigma_-] \\ &= -2(\hat{a}[\sigma_+, \hat{a}^\dagger \sigma_-] + [\hat{a}, \hat{a}^\dagger \sigma_-] \sigma_+) \\ &= -2(\hat{a} \hat{a}^\dagger [\sigma_+, \sigma_-] + [\hat{a}, \hat{a}^\dagger] \sigma_- \sigma_+) \\ &= -2(\hat{a} \hat{a}^\dagger \sigma_z + (\mathbb{1} - \sigma_z)/2) \\ &= -2(\hat{a}^\dagger \hat{a} \sigma_z + (\mathbb{1} + \sigma_z)/2) \\ &= -2(\hat{a}^\dagger \hat{a} + (\mathbb{1} + \sigma_z)/2) \sigma_z \\ &= -2\hat{N}_a \sigma_z, \end{aligned} \quad (51)$$

whereas the second one follows as

$$\begin{aligned} [I_-, \sigma_x] &= [\hat{a}^\dagger \sigma_- - \hat{a} \sigma_+, \sigma_- + \sigma_+] \\ &= -\hat{a}[\sigma_+, \sigma_-] + \hat{a}^\dagger[\sigma_-, \sigma_+] \\ &= -(\hat{a} + \hat{a}^\dagger) \sigma_z. \end{aligned}$$

Upon substitution of these first-order corrections and introduction of the shifted harmonic oscillator operators we get the effective Hamiltonian given in equation (23).

-
- * To whom correspondence should be addressed. Electronic address: alexander.lopez@physik.uni-regensburg.de
- ¹ K. S. Novoselov, A. K. Geim, S. V. Morozov, D. Jiang, Y. Zhang, S. V. Dubonos, I. V. Grigorieva and A. A. Firsov, *Science* **306**, 666 (2004)
- ² A. K. Geim and K. S. Novoselov, *Nature Mater.* **6**, 183 (2007)
- ³ A. H. Castro Neto, F. Guinea, N. M. R. Peres, K. S. Novoselov and A. K. Geim, *Rev. Mod. Phys.* **81**, 109 (2009)
- ⁴ T. Oka and H. Aoki, *Phys. Rev. B* **79**, 081406(R) (2009)
- ⁵ H. L. Calvo, H. M. Pastawski, S. Roche and L. E. F. Foa Torres, *Appl. Phys. Lett.* **98**, 232103 (2011)
- ⁶ Y. Zhou and M. W. Wu, *Phys. Rev. B* **83**, 245436 (2011)
- ⁷ J. Karch, P. Olbrich, M. Schmalzbauer, C. Zoth, C. Brinsteiner, M. Fehrenbacher, U. Wurstbauer, M. M. Glazov, S. A. Tarasenko, E. L. Ivchenko, D. Weiss, J. Eroms, R. Yakimova, S. Lara-Avila, S. Kubatkin, and S. D. Ganichev, *Phys. Rev. Lett.* **105**, 227402 (2010)
- ⁸ C. L. Kane and E. J. Mele, *Phys. Rev. Lett.* **95**, 226801 (2005)
- ⁹ T. Kitagawa, E. Berg, M. Rudner and E. Demler, *Phys. Rev. B* **82**, 235114 (2010)
- ¹⁰ T. Kitagawa, T. Oka, A. Brataas, L. Fu, and E. Demler, *Phys. Rev. B* **84**, 235108 (2011)
- ¹¹ Z. Gu, H. A. Fertig, D. P. Arovas and A. Auerbach, *Phys. Rev. Lett.* **107**, 216601 (2011)
- ¹² B. Dóra, K. Ziegler, P. Thalmeier and M. Nakamura, *Phys. Rev. Lett.* **102**, 036803 (2009)
- ¹³ T. M. Rusin and W. Zawadzki, *Phys. Rev. B* **80**, 045416 (2009)
- ¹⁴ M. Mecklenburg and B. C. Regan, *Phys. Rev. Lett.* **106**, 116803 (2011)
- ¹⁵ J. Cayssol, B. Dóra, F. Simon and R. Moessner, *Phys. Status Solidi RRL* **7**, 101 (2013)
- ¹⁶ M. Grifoni and P. Hänggi, *Physics Reports* **304**, 229 (1998)
- ¹⁷ Q.-g. Lin, *J. Phys. A: Math. Gen.* **34**, 1903 (2001)
- ¹⁸ D. S. L. Abergel and T. Chakraborty, *Nanotech.* **22**, 015203 (2011)
- ¹⁹ R. W. Robinett, *Physics Reports* **92**, 1 (2004); V. Krueckl and T. Kramer, *New J. Phys.* **11**, 093010 (2009); E. Romera and F. de los Santos, *Phys. Rev. B* **80**, 165416 (2009); E. Romera, *Phys. Rev. A* **84**, 052102 (2011)
- ²⁰ A. Voje, J. M. Kinaret and A. Isacsson, *Phys. Rev. B* **85**, 205415 (2012)
- ²¹ D. Leibfried, E. Knill, S. Seidelin, J. Britton, R. B. Blakestad, J. Chiaverini, D. Hume, W. M. Itano, J. D. Jost, C. Langer, R. Ozeri, R. Reichle, and D. J. Wineland, *Nature*, 639 (2005)
- ²² J. Schliemann, *New J. Phys* **10**, 043024 (2008)